PNAS RESEARCH ARTICLE | IMMUNOLOGY AND INFLAMMATION

SEC61G assists *EGFR*-amplified glioblastoma to evade immune elimination

Kunlin Zeng[a,1], Yu Zeng[a,1], Hongchao Zhan[a,1], Ziling Zhan[a], Li Wang[a], Yuxin Xie[a], Yanqing Tang[a], Cuiying Li[a], Yanwen Chen[a], Shangbiao Li[a,b], Ming Liu[a], Xiaoxia Chen[a], Li Liang[c], Fan Deng[a], Ye Song[d], and Aidong Zhou[a,b,c,2]

Edited by William Weiss, University of California, San Francisco; received March 3, 2023; accepted July 6, 2023 by Editorial Board Member Rakesh K. Jain

Amplification of chromosome 7p11 (7p11) is the most common alteration in primary glioblastoma (GBM), resulting in gains of epidermal growth factor receptor (*EGFR*) copy number in 50 to 60% of GBM tumors. However, treatment strategies targeting EGFR have thus far failed in clinical trials, and the underlying mechanism remains largely unclear. We here demonstrate that *EGFR* amplification at the 7p11 locus frequently encompasses its neighboring genes and identifies SEC61G as a critical regulator facilitating GBM immune evasion and tumor growth. We found that *SEC61G* is always coamplified with *EGFR* and is highly expressed in GBM. As an essential subunit of the SEC61 translocon complex, SEC61G promotes translocation of newly translated immune checkpoint ligands (ICLs, including PD-L1, PVR, and PD-L2) into the endoplasmic reticulum and promotes their glycosylation, stabilization, and membrane presentation. Depletion of SEC61G promotes the infiltration and cytolytic activity of $CD8^+$ T cells and thus inhibits GBM occurrence. Further, SEC61G inhibition augments the therapeutic efficiency of EGFR tyrosine kinase inhibitors in mice. Our study demonstrates a critical role of SEC61G in GBM immune evasion, which provides a compelling rationale for combination therapy of *EGFR*-amplified GBMs.

SEC61G | EGFR | PD-L1 | glioblastoma | immune evasion

Glioblastoma (GBM), which accounts for more than 60% of all newly diagnosed glioma cases, is the most malignant and devastating form of primary brain tumor (1). Approximately 50% of GBM cases have epidermal growth factor receptor (*EGFR*) amplification, and half of *EGFR*-amplified tumors express the mutant receptor EGFRVIII, which leads to constitutive activation of the receptor in a ligand-independent manner (2). Despite compelling evidence of EGFR addiction in experimental models, the clinical utility of EGFR tyrosine kinase inhibitors (EGFR-TKIs) in the treatment of GBM remains limited (3). Multiple genetic resistance mechanisms may cause GBM cells to evade EGFR-TKIs, including high cellular heterogeneity of GBM (4), insufficient brain penetration for effective therapy due to the blood–brain barrier (BBB) (5), and compensatory activation of other tumorigenic signaling pathways by EGFR inhibition (6), etc.

GBM is a highly immunosuppressive tumor characterized by low $CD8^+$ T cell infiltration and increased T cell dysfunction (7, 8). Immune checkpoint ligands (ICLs), such as PD-L1 and PVR, are highly expressed in GBM cells and bind to immune checkpoint receptors (ICRs, PD-1, and TIGIT, respectively) on $CD8^+$ T cells, resulting in inhibition of T cell proliferation, production of proinflammatory cytokines, and cytolytic activity (7, 9). ICLs are highly glycosylated, which critically maintains their protein stability and is required for their interaction with ICRs (10–12). Monoclonal antibodies blocking these inhibitory pathways reactivate $CD8^+$ T cells and represent promising immunotherapies for GBM (7). Uncovering the underlying mechanism of ICL regulation will help to develop immunotherapies that improve response rates and survival in GBM patients.

Genomic amplification of oncogenes or deletion of tumor suppressors often encompasses the neighboring genes that cooperatively contribute to tumor initiation and development, making cancer cells highly susceptible to the target therapies of those genes (13–15). By analyzing the *EGFR* gene locus on chromosome 7p11 (7p11), we identified *SEC61G* as one such gene that is most frequently coamplified with *EGFR* and overexpressed in GBM. SEC61G is an essential subunit of the SEC61 translocon complex, which mediates the translocation of secreted and membrane proteins through the endoplasmic reticulum (ER) for further processing (16). We found that SEC61G promotes the translocation of ICLs, including PD-L1, PVR, and PD-L2, into the ER, inducing their N-glycosylation, stabilization, and membrane presentation. Depletion of SEC61G renders GBM cells susceptible to $CD8^+$ T cell–mediated cytotoxicity and inhibits GBM tumorigenesis. Thus, SEC61G

Significance

EGFR (epidermal growth factor receptor) amplification is frequent in primary glioblastoma (GBM); however, targeting EGFR alone is usually inefficient in clinical trials, and the underlying mechanisms remain largely unclear. Here, we revealed that *SEC61G*, an *EGFR* neighboring gene, is frequently coamplified with *EGFR* and is highly expressed in GBM. SEC61G promotes the glycosylation, stabilization, and membrane presentation of immune checkpoint ligands (ICLs) and thus promotes immune evasion and tumorigenesis. Inhibition of SEC61G induces an antitumor immune response and arguments the efficiency of EGFR inhibitor. Thus, SEC61G-mediated immune evasion may act as a critical mechanism for tumorigenesis, especially in *EGFR*-amplified tumors, and targeting SEC61G represents a potential strategy for combination therapy of *EGFR*-amplified GBMs.

Author contributions: A.Z. designed research; K.Z., Y.Z., H.Z., Z.Z., L.W., and Y.X. performed research; Y.T., C.L., Y.C., S.L., M.L., X.C., L.L., F.D., and Y.S. analyzed data; and A.Z. wrote the paper.

The authors declare no competing interest.

This article is a PNAS Direct Submission. W.W. is a guest editor invited by the Editorial Board.

[1]K.Z., Y.Z., and H.Z. contributed equally to this work.

[2]To whom correspondence may be addressed. Email: aidern0927@smu.edu.cn.

This article contains supporting information online at https://www.pnas.org/lookup/suppl/doi:10.1073/pnas.2303400120/-/DCSupplemental.

Published July 31, 2023.

may play a critical role for immune evasion and tumorigenesis of *EGFR*-amplified GBMs, and targeting SEC61G represents a therapeutic strategy for the treatment of those tumors.

Results

Screening of *EGFR* Neighboring Genes at 7p11 Loci Identifies SEC61G as a Key Regulator of Cytotoxic T Cell Activity. It has been shown that *EGFR* amplification in GBM or lung cancer renders tumor insensitive to EGFR-TKIs (3, 17), but the underlying mechanism remains largely unclear. Extensive analysis of cancer genomics indicated that amplification of oncogenes or deletion of tumor suppressors often encompasses the neighboring genes, which cooperatively contribute to tumorigenesis (13–15). We supposed that the *EGFR* neighboring genes on 7p11 may be implicated in tumorigenesis and render *EGFR*-amplified tumors insensitive to EGFR-TKIs. The 7p11 amplicon spans an approximately 6.2-Mb region, in which 17 protein-coding genes exhibited amplification profiles similar to *EGFR*, but to different extents (Fig. 1*A* and *SI Appendix*, Fig. S1*A*). To determine the potential roles of *EGFR* neighboring genes in the occurrence of GBM, we developed an algorithm to analyze the correlation between the amplification of neighboring genes and survival of GBM patients using the TCGA datasets. We found that amplification of the neighboring genes predicted poorer survival in *EGFR*-amplified GBMs (Fig. 1*B*), suggesting that those genes may be implicated in GBM tumorigenesis independently of EGFR.

To identify other potential tumor drivers at the 7p11 loci, we performed a siRNA-based functional screening. siRNA pools (3 siRNAs per gene) targeting those genes were transfected into the patient-derived GBM0108 cells, respectively, and the cells were then cocultured with activated T cells (Fig. 1*C*). We found that transfection of siRNAs against *EGFR*, *SEC61G*, and *MRPS17* efficiently inhibited the growth of GBM cells (Fig. 1*D*). However, among those three genes, transfection of siRNAs against *SEC61G* most significantly inhibited cell viability after cells were cocultured with $CD8^+$ T cells for 48 h (Fig. 1*D*), suggesting that SEC61G represses the cytolytic activity of $CD8^+$ T cells, and was therefore selected for further investigation. Depletion of SEC61G robustly decreased GBM cell viability and increased cell death in the presence of activated T cells as determined by calcein-AM/PI double staining (Fig. 1 *E* and *F*). The effect of SEC61G depletion on $CD8^+$ T cell–mediated killing of cancer cells was validated by crystal violet staining (Fig. 1*G* and *SI Appendix*, Fig. S1*B*). Moreover, we found that the population of granzyme B (GZMB)-expressing $CD8^+$ T cells was increased significantly after SEC61G depletion in GBM cells (Fig. 1*H* and *SI Appendix*, Fig. S1*C*), further confirming the role of SEC61G in regulating cytotoxic T lymphocyte activity.

We next analyzed the clinical relevance between *SEC61G* expression and immune cell infiltration in GBM. GSEA of the TCGA-GBM datasets showed that *SEC61G* levels were negatively correlated with the populations of total T cells and activated $CD8^+$ T cells (Fig. 1*I*) but not with other types of immune cells, such as activated B cells, activated dendritic cells (DC), and activated $CD4^+$ T cells (*SI Appendix*, Fig. S1*D*). Further, in human GBM tissues, the protein levels of SEC61G were negatively correlated with the infiltration and cytolytic activity of $CD8^+$ T cells (Fig. 1*J*). Collectively, these results demonstrate that SEC61G negatively regulates antitumor $CD8^+$ T cell activity against GBM cells.

***SEC61G* Is Coamplified with *EGFR* and Is Highly Expressed in GBM.** Pancancer analysis of TCGA datasets demonstrated that *SEC61G* gene amplification is common in many tumor types, of which GBM is most frequent (~36%) (Fig. 2*A*). In GBM tumors, the levels of *SEC61G* mRNA were positively correlated with the *SEC61G* DNA copy number (Fig. 2*B*). Thus, *SEC61G* mRNA is significantly higher in *SEC61G*-amplified tumors compared with neutral tumors (Fig. 2*C*). Further, SEC61G expression is higher in high-grade gliomas than in low-grade gliomas (*SI Appendix*, Fig. S2*A*), and amplification of *SEC61G* in GBM predicted poor overall survival and disease-free survival (*SI Appendix*, Fig. S2*B*).

Of those genes on 7p11, *SEC61G* is one of the most frequently coamplified genes with *EGFR* (*SI Appendix*, Fig. S1*A*). Over 70 % of GBM cases showing *EGFR* amplification also contain *SEC61G* amplification (Fig. 2*D*). To validate the coamplification of *SEC61G* and *EGFR* in GBM, we examined their DNA copy number in a panel of commercial and patient-derived GBM cells. In most patient-derived GBM cells, we detected an increase of the *SEC61G* copy number to varying degrees, including GBM0108 and GBM0709 cells (Fig. 2*E*). Moreover, in most GBM cells, *EGFR* amplification was accompanied by a gain of *SEC61G* copy number (Fig. 2*E*). Accordingly, the mRNA levels of *SEC61G* and *EGFR* were significantly increased in the cells with genomic amplification and positively correlated with each other in those cells (Fig. 2 *E* and *F*). The positive correlation between SEC61G and EGFR proteins was further confirmed by immunoblotting (Fig. 2*G*).

We next analyzed the clinical relevance between SEC61G and EGFR in GBM. TCGA-GBM datasets revealed that *SEC61G* expression was positively correlated with *EGFR* mRNA levels (Fig. 2*H*). In a serial section of 64 human GBM specimens (WHO grade IV), the protein levels of SEC61G are significantly correlated with EGFR ($r = 0.92$, $P < 0.0001$) (Fig. 2*I*). To examine the correlation between *SEC61G* amplification and the T cell cytolytic activity, GBM cells were cocultured with $CD8^+$ T cells. We found that GBM0108 and GBM0709 cells, which were shown to harbor *SEC61G* amplification, were more resistant to T cell–mediated cell killing than the LN229 and GBM1226 cells, which are *SEC61G* normal (Fig. 2*J*). Accordingly, SEC61G overexpression in LN229 and GBM1226 cells reduced $CD8^+$ T cell–mediated cell killing (*SI Appendix*, Fig. S2 *C–E*). Together, these results strongly support that *SEC61G* is coamplified with *EGFR* and is highly expressed in GBM.

Depletion of SEC61G Diminishes GBM Growth by Restoring $CD8^+$ T Cell Antitumor Immunity. Considering the important role of SEC61G in regulating cytolytic T cell activity, we next examined the effects of SEC61G depletion on GBM tumor formation. We first detected the expression of EGFR and SEC61G in GL-26 and CT-2A mouse GBM cells and found that their levels were higher in GL-26 cells than in GBM1226 and LN229 cells, but relatively lower than the *EGFR*-amplified GBM cells, such as GBM0709 (*SI Appendix*, Fig. S3*A*). However, the copy numbers of *EGFR* and *SEC61G* were normal in GL-26 cells compared with normal mouse fibroblasts (*SI Appendix*, Fig. S3*B*). GL-26 cells expressing *SEC61G* shRNAs were intracranially implanted into immunocompetent C57BL/6 or immunodeficient nude (nu/nu) mice (*SI Appendix*, Fig. S3*C*). We found that depletion of SEC61G strongly inhibited tumor growth in C57BL/6 mice (Fig. 3 *A* and *C*) but had only a marginal effect in nude (nu/nu) mice (Fig. 3 *B* and *C*), indicating a critical involvement of T cell–mediated immune surveillance in tumor suppression. Consistently, depletion of SEC61G significantly prolonged the survival of C57BL/6 mice (medium survival duration of 20 d in control vs. 42 d in sh1 and 40 d in sh2) but only moderately affected the survival of the nude mice (15 d vs. 25 d and 23 d, respectively) (Fig. 3*D*).

To assess the effect of SEC61G depletion on antitumor immunity, brain tissues from GL-26 GBM-bearing C57BL/6 mice were analyzed by flow cytometry. We found that depletion of SEC61G significantly increased the population of $CD8^+$ T cells ($CD8^+CD3^+$) and induced cytotoxic $CD8^+$ T cell activation ($GZMB^+CD8^+$)

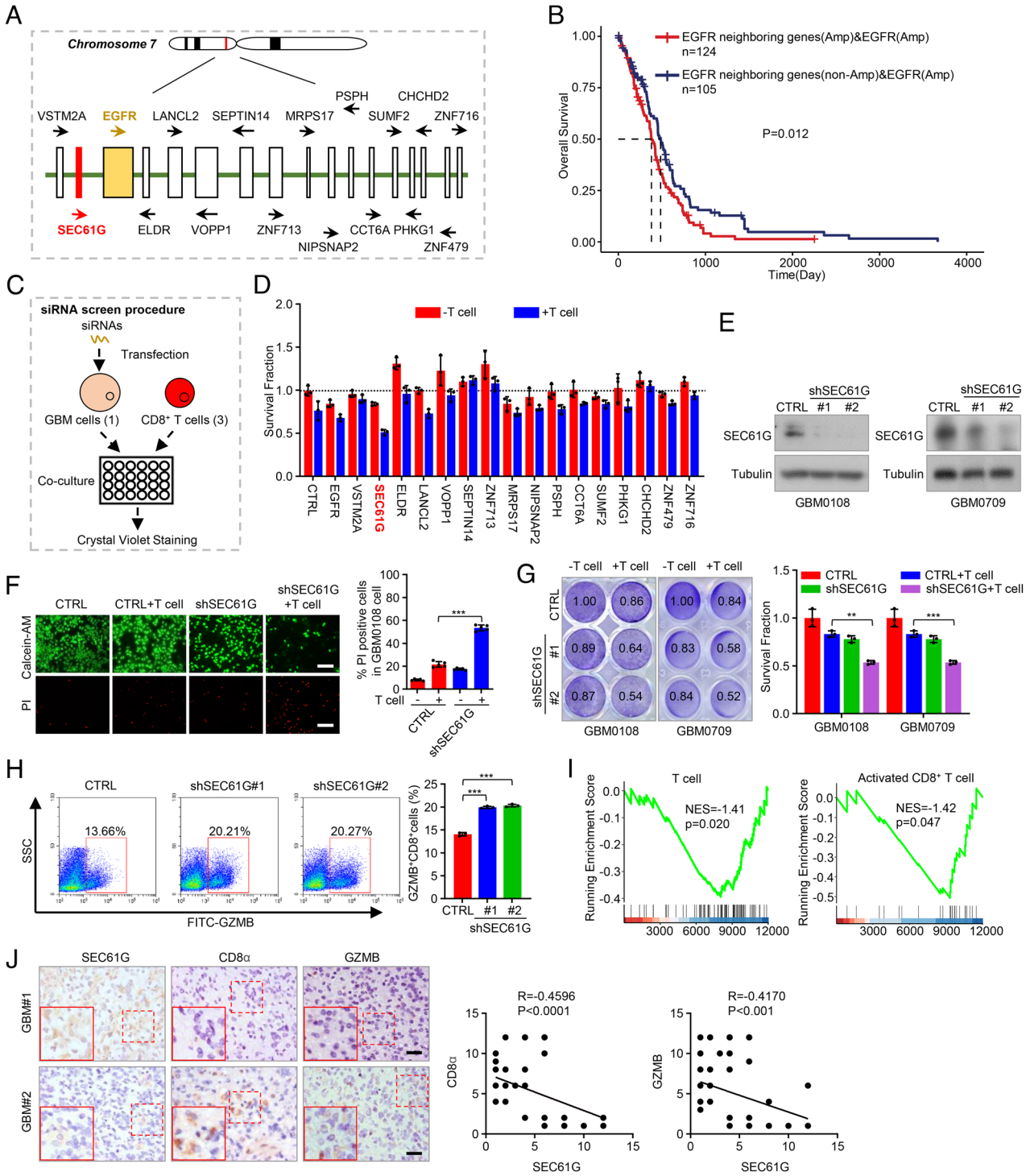

Fig. 1. Screen of genes at 7p11 loci identified SEC61G as a key regulator of cytolytic T cell activity. (*A*) Sketch showing the gene arrangement on chromosome 7p11 amplicon. (*B*) TCGA-GBM datasets demonstrated the correlation between *EGFR* neighboring gene amplification and prognosis of GBM patients in *EGFR*-amplified tumors. Samples were classified into two groups: "*EGFR* neighboring genes (Amp) and *EGFR* (Amp)" based on *EGFR* amplification and *EGFR* neighboring genes all amplification; and "*EGFR* neighboring genes (non-Amp) and *EGFR* (Amp)" based on *EGFR* amplification and *EGFR* neighboring genes not all amplification. (*C*) Diagram showing the procedure of siRNA screen strategy. (*D*) The patient-derived GBM0108 cells were transfected with siRNA pools against different genes and then cocultured with activated T cells for 48 h (effect-target ratio: 3:1). The surviving GBM cells were stained with crystal violet, and relative fold ratios of surviving cells were calculated (mean ± SEM, n = 3 independent assays). (*E*) GBM0108 and GBM0709 cells stably expressing *SEC61G* shRNAs were lysed and then subjected to immunoblotting. (*F*) GBM0108 cells expressing *SEC61G* shRNAs were cocultured with activated T cells for 48 h (E-T ratio, 3:1). The surviving and dead cells were detected by calcein-AM/PI costaining. Representative images were shown. The percentage of PI-positive cells was counted (mean ± SEM, n = 5 randomly selected microscope fields). ***$P < 0.001$. (*G*) GBM0108 and GBM0709 cells expressing *SEC61G* shRNAs were cocultured with activated T cells for 48 h (E-T ratio, 3:1). The surviving cells were stained with crystal violet, and relative fold ratios of surviving cells were calculated (mean ± SEM, n = 3 independent assays). **$P < 0.01$, ***$P < 0.001$. (*H*) After cell coculture, the T cells in (*G*) were subjected to FACS analysis. Representative flow cytometry plots and statistical quantitation of $GZMB^+CD8^+$ TILs are shown (mean ± SEM, n = 3 independent experiments). ***$P < 0.001$. (*I*) GSEA shows the correlation between *SEC61G* expression and the levels of total T cells or activated $CD8^+$ T cells in GBM. (*J*) Consecutive GBM tissues were immunostained with anti-SEC61G, anti-CD8α, and anti-GZMB antibodies, respectively. Representative images of two tumors are shown. (Scale bars, 100 μm.) The correlation of SEC61G, CD8α, and GZMB levels was statistically significant among different specimens (n = 64 GBM tissues, SEC61G vs. CD8α, r = −0.4596, $P < 0.0001$; SEC61G vs. GZMB, r = −0.4170, $P < 0.001$, Pearson correlation test). Note that the scores of some samples overlap.

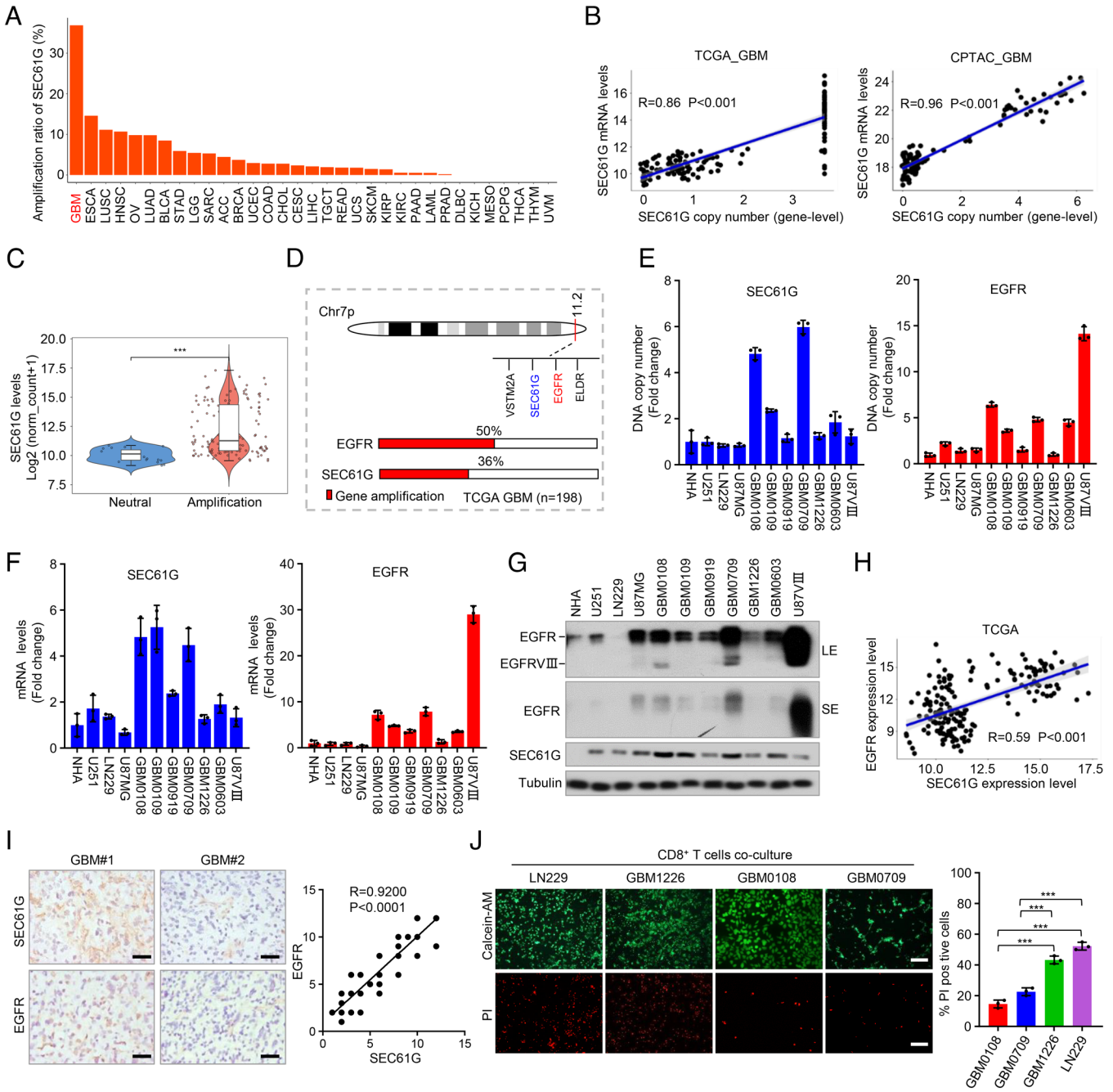

Fig. 2. *SEC61G* is coamplified with *EGFR* and is highly expressed in GBM. (*A*) Frequency of *SEC61G* amplification in different kinds of cancers from the TCGA datasets. (*B*) The correlation between *SEC61G* copy number and the mRNA levels from the TCGA-GBM and CPTAC-GBM datasets. (*C*) TCGA dataset indicates that the mRNA levels of *SEC61G* in *SEC61G*-amplified GBMs are significantly higher than the nonamplification tumors. (*D*) A schematic diagram shows the coamplification of *SEC61G* with *EGFR* in GBM. (*E*) Genomic DNA of different GBM cells was extracted, and the DNA copy numbers of *EGFR* and *SEC61G* were quantified by RT-PCR using specific primers (exon 9 to 10 of *EGFR*, and exon 3 to 4 of *SEC61G*). *GAPDH* was used as an internal control. Values were normalized to NHA (mean ± SEM, n = 3 independent experiments). (*F*) The mRNA levels of *EGFR* and *SEC61G* in GBM cells were quantified by RT-PCR using specific primers. *GAPDH* was used an internal control. Values were normalized to NHA (mean ± SEM, n = 3 independent experiments). (*G*) Immunoblotting analysis of EGFR and SEC61G in NHA, human GBM cells (LN229, U251, U87MG, and U87-EGFR*VIII*), and the patient-derived GBM cells (GBM0108, GBM0109, GBM0919, GBM0709, GBM1226, and GBM0603). LE, long exposure. SE, short exposure. (*H*) The correlation between *SEC61G* and *EGFR* mRNA levels in GBM from the TCGA datasets. (*I*) Consecutive GBM tissues were immunostained with anti-SEC61G and anti-EGFR antibodies, respectively. Representative images of two tumors are shown (*Left*). (Scale bars, 100 μm.) The correlations of SEC61G and EGFR expression levels were statistically significant among different specimens (n = 64 tumors, r = 0.9200, $P < 0.0001$, Pearson correlation test). Note that the scores of some samples overlap (*Right*). (*J*) GBM cells were cocultured with activated T cells, and the surviving and dead cells were detected by calcein-AM/PI double staining. Representative images are shown. Data are expressed as mean ± SEM of n = 3 independent assays. ***$P < 0.001$.

(Fig. 3*E* and *SI Appendix*, Fig. S3*D*). Immunostaining of mouse tissues demonstrated that SEC61G depletion inhibited the expression of PD-L1, a critical immune checkpoint molecule expressed in tumor cells (Fig. 3*F*). The stimulatory effect of SEC61G depletion on $CD8^+$ T cell infiltration and cytotoxic activity were further confirmed by double staining of CD8α and GZMB in mouse tissues (Fig. 3*G*). To clarify whether SEC61G depletion inhibits tumor growth by inducing antitumor $CD8^+$ T cell immunity, GL-26 GBM-bearing mice were treated with an anti-CD8α monoclonal antibody (mAb). Compared with IgG2b control mAb, administration of CD8α mAb significantly reversed the effect of SEC61G depletion on tumor growth (Fig. 3*H* and *SI Appendix*, Fig. S3*E*)

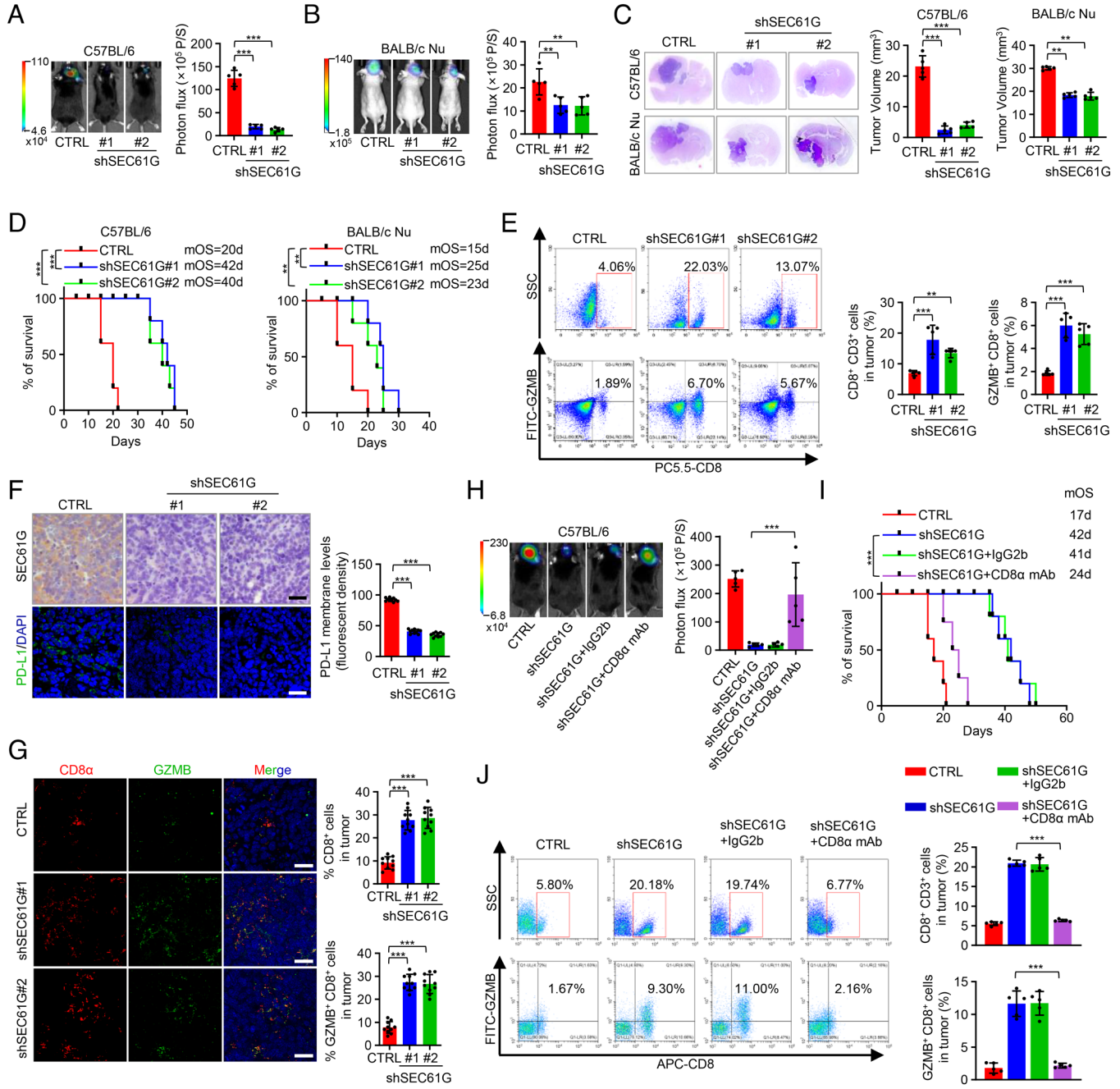

Fig. 3. Depletion of SEC61G inhibits GBM tumorigenesis by enhancing antitumor T cell immunity. (*A* and *B*) GL-26 cells (5 × 10^5 cells/mouse) stably expressing control shRNA or *SEC61G* shRNAs were injected intracranially into C57BL/6 mice (*A*) or BALB/c nude mice (*B*). Tumor growth was monitored by bioluminescence imaging. Representative images are shown, and tumor bioluminescence was quantified (mean ± SD. n = 5 mice for each group, one-way ANOVA test). $^{**}P < 0.01$, $^{***}P < 0.001$. (*C*) Three weeks after injection, the mice were humanely killed, and tumor growth was assessed. The hematoxylin and eosin (H&E)-stained sections show representative tumors. Tumor volumes were calculated (mean ± SD, n = 5 mice for each group, One-way ANOVA test). $^{***}P < 0.001$. (*D*) The survival of mice was evaluated (n = 5 mice for each group, Kaplan–Meier model with a two-sided log-rank test). $^{**}P < 0.01$, $^{***}P < 0.001$. (*E*) Flow cytometry analysis demonstrated the population of $CD8^+$ and $GZMB^+$ $CD8^+$ cells in $CD3^+$ TILs of mouse GBM tissues. Representative plots and quantification of flow cytometry are shown (mean ± SEM, n = 5 independent experiments), $^{**}P < 0.01$, $^{***}P < 0.001$. (*F*) Immunostaining of SEC61G and PD-L1 in mouse GBM tissues. Representative images are shown. (Scale bar, 100 μm.) The intensity of PD-L1 staining was quantified (mean ± SEM, n = 10 randomly selected microscope fields, Student's *t* test). $^{***}P < 0.001$. (*G*) Mouse brain tissues were double stained with CD8α and GZMB. Representative images are shown. (Scale bar, 100 μm.) CD8 and GZMB levels were quantified by ImageJ (mean ± SEM, n = 10 randomly selected fields, Student's *t* test). $^{***}P < 0.001$. (*H*) GL-26 cells (5 × 10^5 cells/mouse) stably expressing control shRNA or *SEC61G* shRNAs were injected intracranially into C57BL/6 mice. Mice were then injected intraperitoneally with CD8α mAb (100 μg/mouse/d) or IgG2b (100 μg/mouse/d). Tumor growth was monitored by bioluminescence imaging. Representative images are shown, and tumor bioluminescence was quantified (mean ± SD. n = 5 mice for each group, one-way ANOVA test). $^{***}P < 0.001$. (*I*) The survival of mice was evaluated (n = 5 mice for each group, Kaplan–Meier model with a two-sided log-rank test). $^{***}P < 0.001$. (*J*) Flow cytometry analysis demonstrated the population of $CD8^+$ and $GZMB^+$ $CD8^+$ cells in $CD3^+$ TILs of mouse GBM tissues. Representative plots and quantification of flow cytometry are shown (mean ± SEM, n = 5 independent assays), $^{***}P < 0.001$.

and accordingly reduced the survival of GBM-bearing mice (42 d in shSEC61G plus IgG2b vs. 24 d in shSEC61G plus CD8α mAb) (Fig. 3*I*). In the mouse GBM tissues, we confirmed that CD8α mAb effectively inhibited $CD8^+$ T cell infiltration and activation, which were induced by SEC61G depletion (Fig. 3*J* and *SI Appendix*, Fig. S3*F*). Collectively, these results suggest that depletion of SEC61G inhibits GBM tumorigenesis by promoting $CD8^+$ T cell infiltration and cytotoxic activity.

SEC61G Induces Glycosylation of Immune Checkpoint Molecules and Inhibits Their Ubiquitination. As an essential subunit of the secretory 61 (SEC61) translocon complex, SEC61G is required for posttranslational modification of most secretory or membrane proteins, including the N-linked glycosylation (18). We first detected the interaction between SEC61G and the ICLs, including PD-L1, PVR, and PD-L2, which have been reported to undergo N-glycosylation for their membrane presentation and functional activities (10–12). Reciprocal immunoprecipitation assays in GBM cells showed that SEC61G indeed interacted with those ICLs (Fig. 4*A* and *SI Appendix*, Fig. S4*A*). To determine the effect of SEC61G on ER translocation of PD-L1, GBM cells were double stained with antibodies against PD-L1 and GRP94, an ER marker. We found that depletion of SEC61G inhibited translocation of PD-L1 into the ER (Fig. 4*B*). Accordingly, depletion of SEC61G significantly decreased the levels of the glycosylated form of PD-L1 and correspondingly increased the levels of the nonglycosylated PD-L1 in GBM cells (Fig. 4*C*).

The N-glycosylation of PD-L1, PVR, and PD-L2 has been shown to critically regulate their polyubiquitination and ER-associated protein degradation (10–12). We next examined the effect of SEC61G on ubiquitination of those ICLs. As expected, overexpression of SEC61G in 293T cells greatly decreased the ubiquitination of PD-L1, PVR, and PD-L2 (Fig. 4*D* and *SI Appendix*, Fig. S4*B*). Consistent with the results, depletion of SEC61G in GBM0108 cells increased the ubiquitination of those ICLs (Fig. 4*E* and *SI Appendix*, Fig. S4*C*). Further, the inhibitory effect of SEC61G on PD-L1 ubiquitination was reversed by tunicamycin (TM) (Fig. 4*F*), a specific inhibitor of N-linked glycosylation, suggesting that SEC61G regulates PD-L1 ubiquitination in an N-glycosylation-dependent manner. Taken together, these results indicate that SEC61G-mediated ER translocation of ICLs promotes their N-glycosylation and inhibits their polyubiquitination.

SEC61G Promotes the Expression and Membrane Localization of ICLs. We next examined the effect of SEC61G on the expression of the ICLs. We found that SEC61G depletion significantly decreased the total levels of PD-L1, PVR, and PD-L2 in GBM0108 and GBM0709 cells (Fig. 5*A*). Likewise, the membrane-bound forms of PD-L1 and PVR were also significantly decreased by SEC61G depletion in GBM cells as determined by flow cytometry (Fig. 5*B* and *SI Appendix*, Fig. S5*A*), and the results were further confirmed by immunostaining (Fig. 5*C* and *SI Appendix*, Fig. S5*B*). Previous studies have shown that SEC61G induces EGFR expression (19). In addition, the EGFR pathway has been reported to up-regulate PD-L1 (20). To determine whether SEC61G induces PD-L1 expression through EGFR, GBM cells with SEC61G depletion were treated with EGF. We found that SEC61G depletion did moderately down-regulate EGFR levels and repressed the EGFR pathway in GBM cells (*SI Appendix*, Fig. S5*C*). However, EGF only marginally reversed the effect of SEC61G depletion on PD-L1 expression (*SI Appendix*, Fig. S5*D*), indicating that SEC61G induces the PD-L1 expression mostly independent of EGFR.

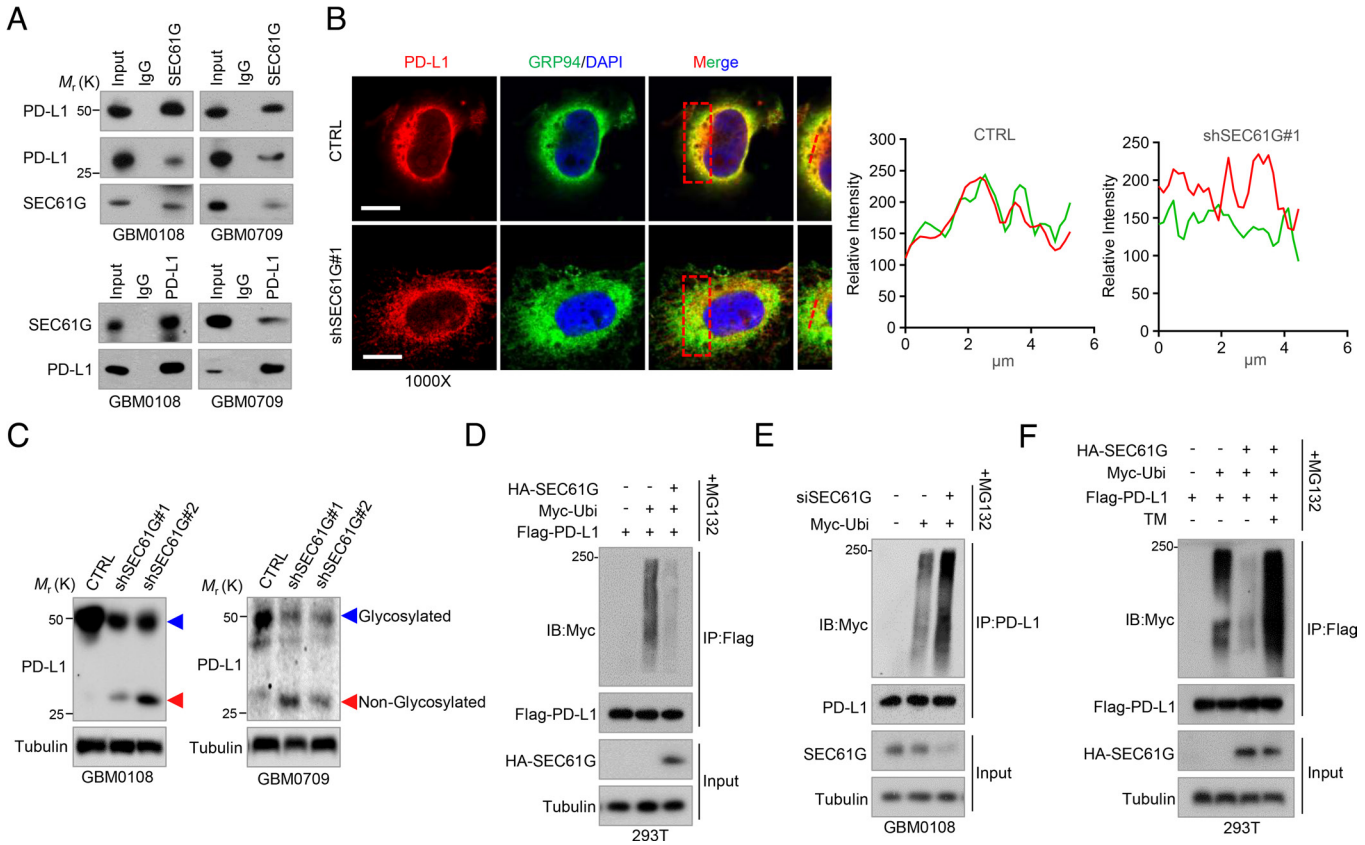

Fig. 4. SEC61G induces N-glycosylation of the ICLs and inhibits their ubiquitination. (*A*) Reciprocal interaction between SEC61G and PD-L1 in GBM0108 and GBM0709 cells. (*B*) GBM0108 cells expressing control shRNA or *SEC61G* shRNA were double stained with anti-PD-L1 and anti-GRP94 antibodies. *Insets*: High-magnification images. (Scale bars, 10 μm.) Line scan of the relative fluorescence intensity of the signal, demonstrating peak overlapping (*Right*). (*C*) GBM0108 and GBM0709 cells expressing *SEC61G* shRNAs were subjected to immunoblotting using an anti-PD-L1 antibody. The blue and red arrows indicate glycosylated and nonglycosylated PD-L1, respectively. (*D*) 293T cells were transfected with Flag-PD-L1, Myc-Ubi, and HA-SEC61G and then treated with MG132 for 6 h. Cell lysates were immunoprecipitated using an anti-Flag antibody and then analyzed by immunoblotting. (*E*) GBM0108 cells were transfected with *SEC61G* siRNA and Myc-Ubi and then treated with MG132 for 6 h. Cell lysates were immunoprecipitated using an anti-PD-L1 antibody and then analyzed by immunoblotting. (*F*) 293T cells were transfected with Flag-PD-L1, HA-SEC61G, and Myc-Ubi and then treated with 5 μg/mL TM for 12 h in the presence of MG132. Cell lysates were immunoprecipitated using an anti-Flag antibody and then analyzed by immunoblotting using the indicated antibodies.

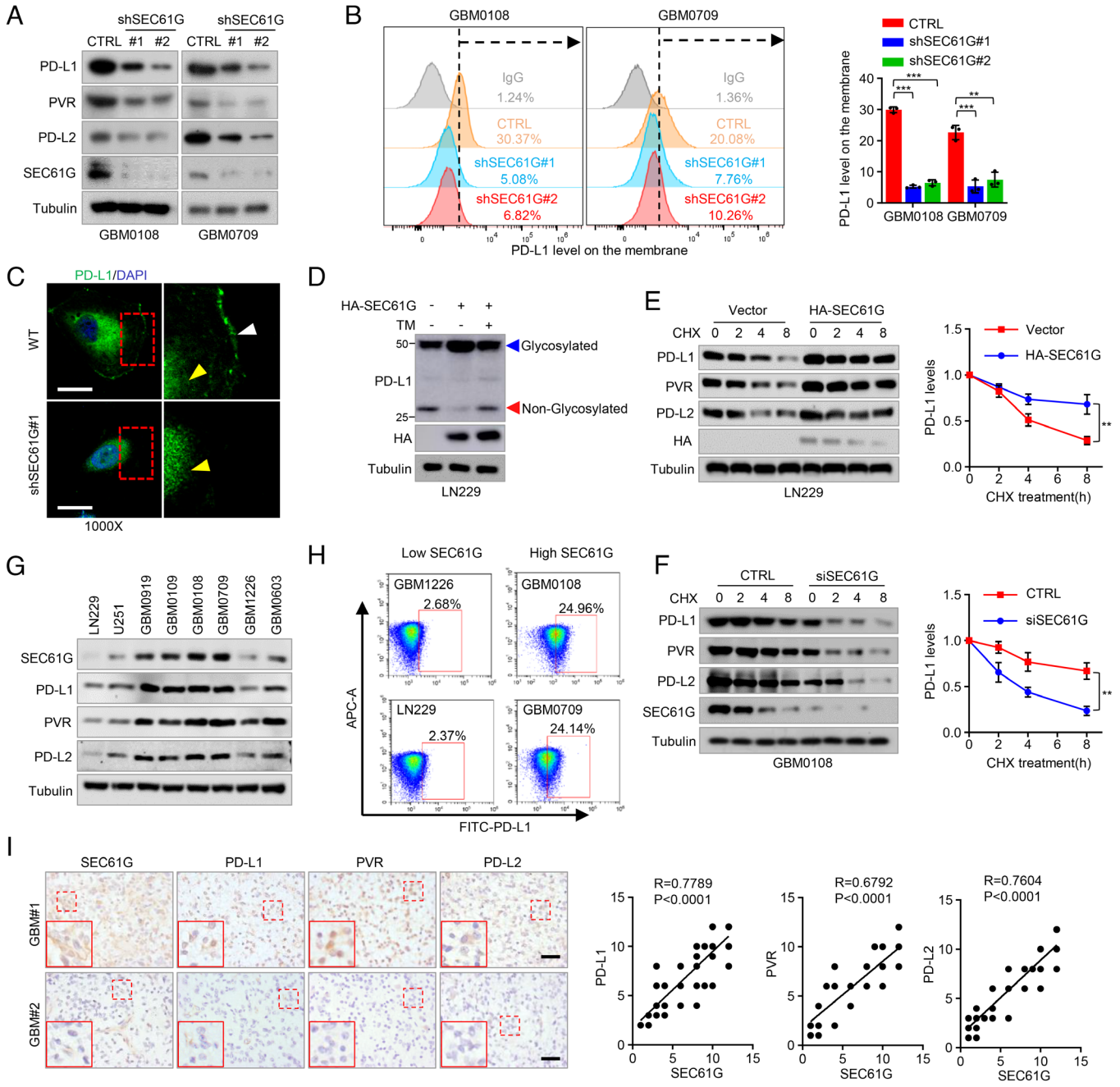

Fig. 5. SEC61G promotes the stability and membrane localization of immune checkpoint molecules. (*A*) GBM0108 and GBM0709 cells expressing *SEC61G* shRNAs were analyzed by immunoblotting using antibodies against the indicated ICLs. (*B*) The levels of membrane-bound PD-L1 in GBM0108 and GBM0709 cells expressing *SEC61G* shRNAs were analyzed by FACS. Representative plots and quantification of flow cytometry are shown (mean ± SEM., n = 3 independent experiments). $^{**}P < 0.01$, $^{***}P < 0.001$. (*C*) Immunostaining of PD-L1 in GBM0108 cells expressing control or *SEC61G* shRNA. (Scale bar, 10 μm.) The white and yellow arrows indicate membrane-bound and cytosol PD-L1, respectively. (*D*) LN229 cells were transfected with HA-SEC61G plasmid and then treated with 5 μg/mL TM for 12 h. Cell lysates were analyzed by immunoblotting. (*E* and *F*) GBM0108 cells expressing *SEC61G* shRNA and LN229 cells expressing HA-SEC61G were treated with CHX for the indicated time intervals, and cell lysates were analyzed by immunoblotting. Band intensities of PD-L1 were quantified, and values were expressed as PD-L1 levels relative to untreated cells (mean ± SD., n = 3 independent experiments, paired Student's *t* test, *Right*). $^{**}P < 0.01$. (*G*) The expression of SEC61G, PD-L1, PVR, and PD-L2 in different GBM cells was analyzed by immunoblotting. (*H*) The membrane-bound levels of PD-L1 in the SEC61G-high and SEC61G-low GBM cells were analyzed by flow cytometric assays. (*I*) Consecutive tissue slides of 64 human GBM specimens were immunostained using antibodies against SEC61G, PD-L1, PVR, and PD-L2. Representative images of two tumors are shown. (Scale bars, 100 μm.) The expression correlations between SEC61G and PD-L1, PVR, and PD-L2 were statistically significant among different specimens (n = 64 GBM tumors, SEC61G vs. PD-L1, r = 0.7789; SEC61G vs. PVR, r = 0.6792; SEC61G vs. PD-L2, r = 0.7604; Pearson correlation test, $P < 0.0001$). Note that the scores of some samples overlap.

To determine whether SEC61G regulation of ICLs depends on the N-glycosylation modification, LN229 cells overexpressing SEC61G were treated with TM. As we expected, TM treatment reversed the effect of SEC61G on the expression of ICLs (Fig. 5*D* and *SI Appendix*, Fig. S5*E*). Moreover, SEC61G overexpression in LN229 cells extended the half-life of PD-L1, PVR, and PD-L2 after treatment by cycloheximide (CHX) (Fig. 5*E* and *SI Appendix*, Fig. S5*F*). Accordingly, depletion of SEC61G in GBM0108 cells induced their degradation (Fig. 5*F* and *SI Appendix*, Fig. S5*G*). Because PD-L1 is the most important ICL contributing to cancer immune evasion, we next investigated whether SEC61G promotes GBM tumorigenesis through its regulation of PD-L1. Our results demonstrated that PD-L1 depletion significantly inhibited intracranial tumor growth of GL-26 cells (*SI Appendix*, Fig. S5 *H–J*).

Importantly, while SEC61G depletion substantially inhibited GBM growth and prolonged mouse survival compared with control, further depletion of SEC61G in PD-L1-depleted cells only moderately affected tumor growth and mouse survival (*SI Appendix*, Fig. S5 *H–J*), indicating that SEC61G promotes GBM tumorigenesis, at least partially, through PD-L1.

The regulation of SEC61G on the stability of ICLs suggested clinical relevance of SEC61G with those molecules. In a panel of GBM cells, total protein levels of SEC61G were positively correlated with PD-L1, PVR, and PD-L2, respectively (Fig. 5*G*). Accordingly, the levels of the membrane-bound form of PD-L1 and PVR were significantly higher in cells with high-level SEC61G than those with low SEC61G expression (Fig. 5*H* and *SI Appendix*, Fig. S5*K*). Moreover, in serial sections of 64 GBM specimens, the levels of SEC61G were positively correlated with PD-L1, PVR, and PD-L2 (Fig. 5*I*). Together, these results demonstrate that SEC61G promotes the stability of ICLs and induces their expression in GBM.

SEC61G Inhibition Augments the Efficacy of EGFR-TKIs. We next explored the effect of SEC61G depletion on the efficacy of EGFR-TKIs in GBM treatment. Both erlotinib and lapatinib effectively inhibited the EGFR pathway in mouse GL-26 cells, as in human GBM0108 and GBM0709 cells, and accordingly inhibited cell growth (*SI Appendix*, Fig. S6 *A* and *B*). Using an immunocompetent mouse model of intracranial GBM (Fig. 6*A*), we found that erlotinib alone moderately inhibited GBM growth (Fig. 6 *B* and *C*) and prolonged survival of GL-26 GBM-bearing mice (Fig. 6*D*) (median survival duration of 18 d vs. 30 d). However, treatment with erlotinib in combination with depletion of SEC61G resulted in almost complete suppression of tumor growth (Fig. 6 *B* and *C*) and significant prolongation of

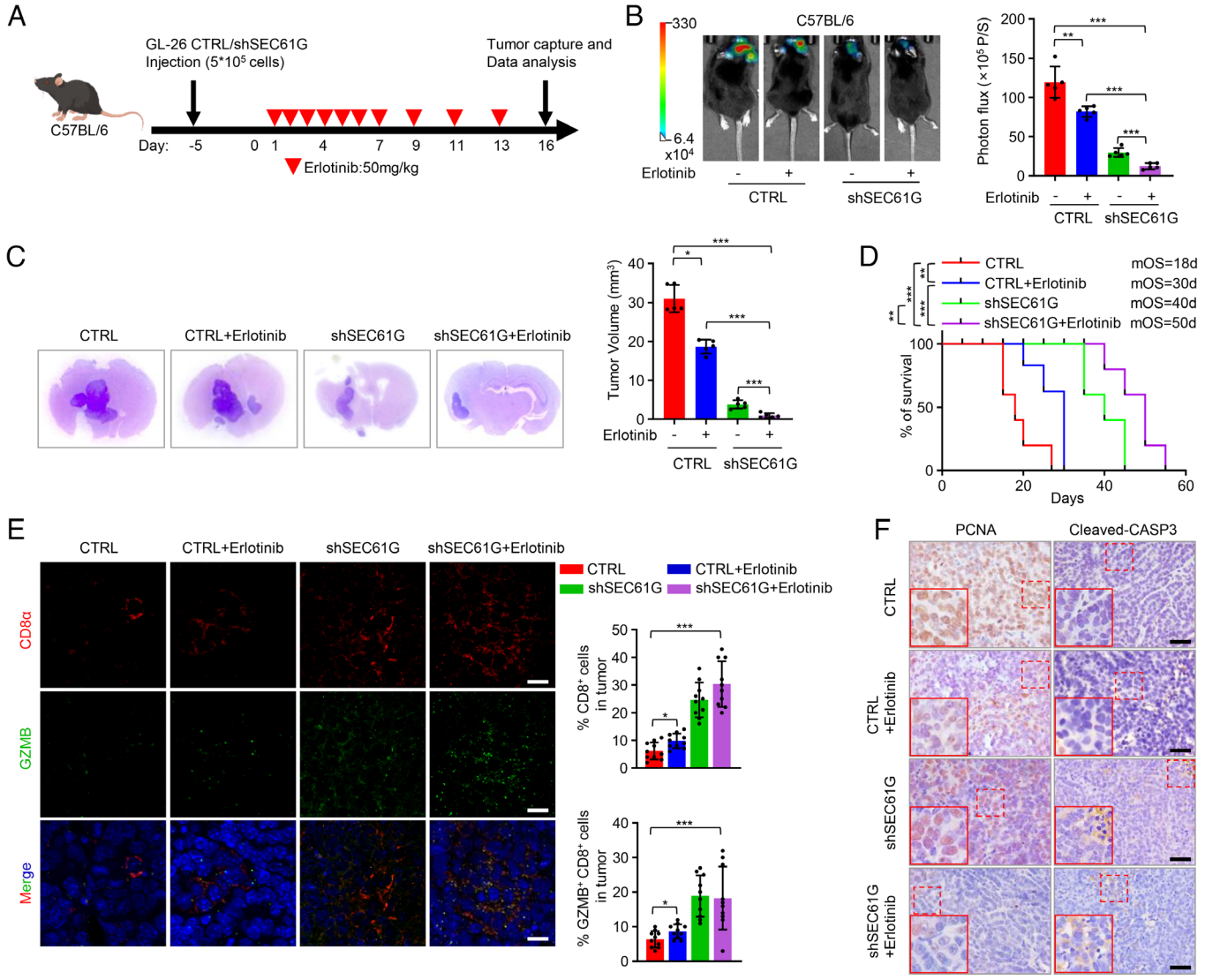

Fig. 6. SEC61G depletion augments the efficacy of erlotinib in an immunocompetent GBM mouse model. (*A*) Schematic representation of mouse treatment schedules. (*B*) GL-26 cells (5 × 10^5 cells/mouse) expressing control or *SEC61G* shRNA were implanted intracranially into C57BL/6 mice. Mice were then injected intraperitoneally with erlotinib (50 mg/kg/d) or vehicle. Tumor growth was monitored by bioluminescence imaging 3 wk after cell implantation. Representative images are shown. Tumor bioluminescence was quantified (mean ± SD, n = 5 mice for each group, one-way ANOVA test). $^{**}P < 0.01$, $^{***}P < 0.001$. (*C*) Three weeks after injection, the mice were humanely killed, and tumor growth was assessed. The H&E-stained sections show representative tumor. Tumor volumes were calculated (mean ± SD, n = 5 mice for each group, One-way ANOVA test). $^{*}P < 0.05$, $^{***}P < 0.001$. (*D*) The survival of mice in (*B*) was evaluated (n = 5 mice for each group, Kaplan–Meier model with a two-sided log-rank test). $^{**}P < 0.01$, $^{***}P < 0.001$. (*E*) The brain tissues of GL-26 GBM-bearing mice were double stained with CD8α and GZMB. Representative images are shown. (Scale bar, 50 μm.) CD8 and GZMB levels were quantified by ImageJ (mean ± SEM, n = 10 randomly selected fields, Student's *t* test). $^{*}P < 0.05$, $^{***}P < 0.001$. (*F*) The mouse brain tissues were immunostained using antibodies against PCNA and cleaved-CASP3. Representative microphotographs are shown. (Scale bar, 100 μm.)

mouse survival (Fig. 6*D*) (18 d vs. 50 d). In mouse GBM tissue, erlotinib in combination with SEC61G depletion significantly increased the infiltration of antitumor CD8$^+$ T cells and the level of cleaved caspase-3, while it decreased the level of PCNA (Fig. 6 *E* and *F*), indicating an increased cell death and inhibition of cell proliferation.

We further investigated the effect of SEC61 blockage on antitumor immunity and GBM growth. Eeyarestatin I (ES I) (Fig. 7*A*),

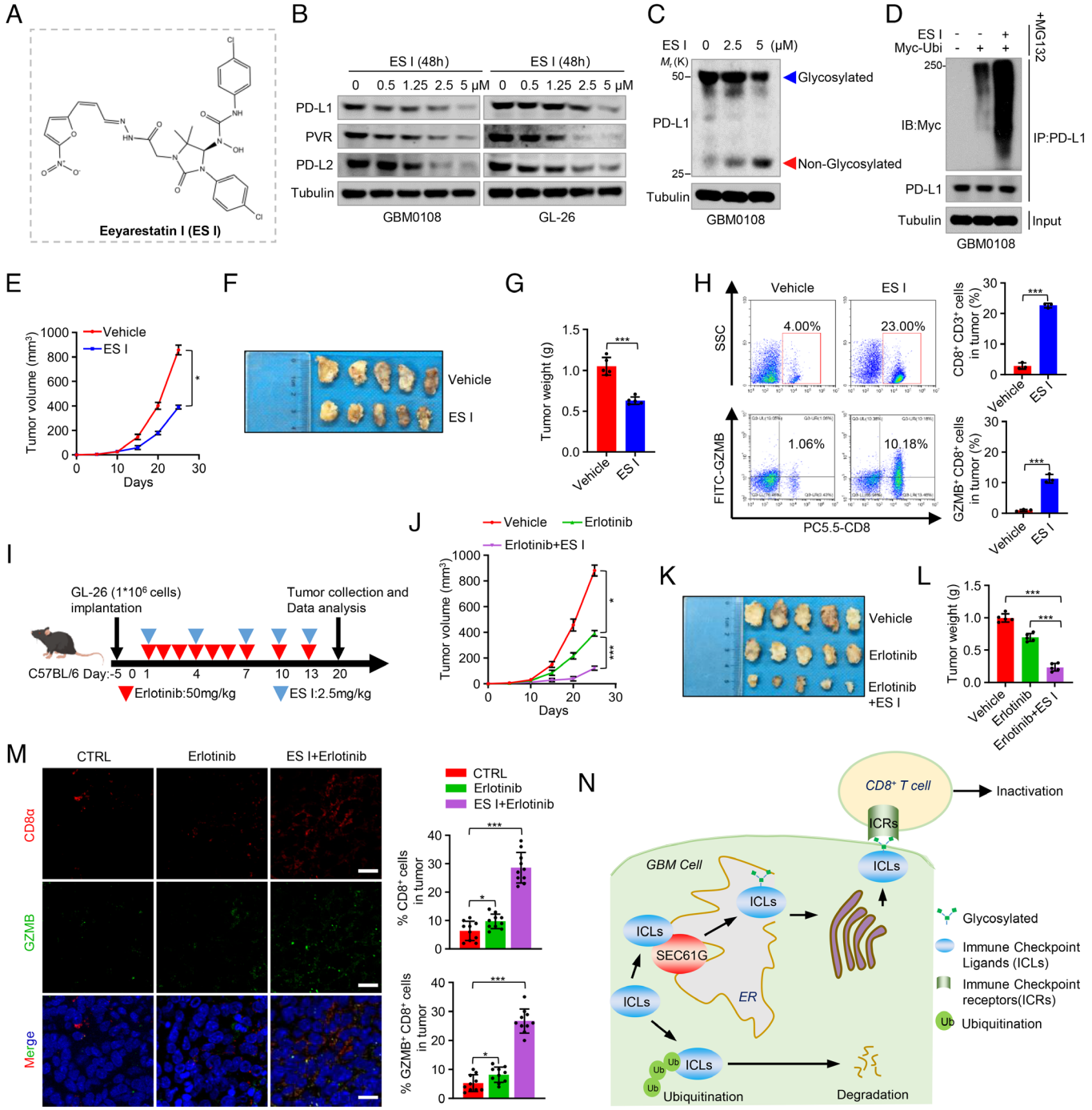

Fig. 7. Eeyarestatin I in combination with erlotinib abolishes tumor growth. (*A*) Chemical structure of Eeyarestatin I (ES I). (*B*) GBM0108 and GL-26 cells were treated with the indicated concentrations of ES I for 48 h. Cell lysates were analyzed by immunoblotting using the indicated antibodies. (*C*) GBM0108 cells were treated with the indicated concentrations of ES I, and the cell lysates were analyzed by immunoblotting using an anti-PD-L1 antibody. (*D*) GBM0108 cells were transfected with Myc-Ubi and then treated with ES I for 48 h in the presence of MG132. Cell lysates were immunoprecipitated using an anti-PD-L1 antibody and then analyzed by immunoblotting. (*E*–*G*) GL-26 cells (1 × 10^6 cells) were injected subcutaneously into C57BL/6 mice and then treated with ES I (2.5 mg/kg). Tumor volume for each time point after injection was calculated (*E*). The resected tumors of each group are shown (*F*), and tumor weight was recorded (*G*). Data are expressed as mean ± SD, n = 5 mice for each group, one-way ANOVA test. *P < 0.05, ***P < 0.001. (*H*) Representative flow cytometry plots and quantification of CD8$^+$ and GZMB$^+$ CD8$^+$ cells in CD3$^+$ TILs in mouse brain tissues (mean ± SEM, n = 5 independent assays). ***P < 0.001. (*I*) Schematic representation of mouse treatment schedules. (*J*–*L*) GL-26 cells (1 × 10^6 cells) were injected subcutaneously into C57BL/6 mice and then treated with erlotinib (50 mg/kg) alone or ES I (2.5 mg/kg) plus erlotinib. The tumor volume for each time point after injection was calculated (*J*). The resected tumors of each group are shown (*K*), and tumor weight was recorded (*L*). Data are expressed as mean ± SD, n = 5 mice for each group, one-way ANOVA test. *P < 0.05, ***P < 0.001. (*M*) The brain tissues were double stained with CD8α and GZMB. Representative images are shown. (Scale bar, 50 μm.) CD8 and GZMB levels were quantified by ImageJ (mean ± SEM, n = 10 randomly selected fields, Student's *t* test). *P < 0.05, ***P < 0.001. (*N*) The diagram shows the findings revealed in this study. *SEC61G* is coamplified with *EGFR* and overexpressed in GBM, which promotes the ER translocation, glycosylation, and stability of the ICLs, resulting in immune evasion and GBM tumorigenesis.

a SEC61 translocon inhibitor, has been shown to inhibit SEC61-mediated protein translocation at the ER (21). ES I has been reported to induce cell death, suppress tumor growth, and sensitize tumors to TKIs in various cancers (22–24). We found that treatment of GBM cells with ES I decreased the levels of PD-L1, PVR, and PD-L2 in a dose-dependent manner (Fig. 7*B*). Moreover, ES I decreased the level of glycosylated PD-L1 in GBM cells (Fig. 7*C*), resulting in increased PD-L1 ubiquitination (Fig. 7*D*). Due to its relatively large molecular size (MW: 630) and potentially low BBB permeability, we used a subcutaneous mouse model to study the role of ES I in tumor growth. Consistent with the above results, ES I substantially inhibited tumor growth (Fig. 7 *E*–*G*). Flow cytometric analysis of tumor tissues confirmed that ES I increased the infiltration and cytolytic activity of the $CD8^+$ T cells (Fig. 7*H* and *SI Appendix*, Fig. S7). Moreover, while erlotinib alone had a moderate effect on tumor growth (Fig. 7 *I*–*L*), ES I in combination with erlotinib almost abrogated tumor formation (Fig. 7 *I*–*L*). In mouse tumor tissues, erlotinib in combination with ES I significantly promoted the infiltration of antitumor $CD8^+$ T cells (Fig. 7*M*). Taken together, these results indicate that SEC61G depletion or inhibition activates antitumor $CD8^+$ T cell immunity and promotes tumor response to EGFR-TKIs, supporting a combinatorial therapeutic strategy for GBM.

Discussion

The ineffectiveness of EGFR-TKIs alone in GBM clinical trials prompts us to consider other mechanisms that contribute to tumorigenesis in *EGFR*-amplified tumors. In this study, we identified *SEC61G* as an *EGFR*-coamplified gene at the 7p11 loci and demonstrated that SEC61G promotes GBM immune evasion by inducing glycosylation, stabilization, and membrane presentation of ICLs (Fig. 7*N*). Thus, targeting SEC61G represents a promising strategy to restore the antitumor immune microenvironment, which provides a compelling rationale for combination therapy of *EGFR*-amplified GBMs.

Although several EGFR-TKIs (including first- and second-generation) have been approved for the treatment of non-small-cell lung cancer, they have shown disappointing results in clinical trials in GBM (3). The reasons that lead to resistance to EGFR-TKIs in GBM are largely unknown, which may include intertumoral heterogeneity, redundancy in signaling pathways, and insufficient brain penetration of the inhibitors due to the BBB (3). It has been shown that amplification of EGFR renders tumor insensitive to EGFR-TKIs (17). Our study demonstrates that *SEC61G* is coamplified with *EGFR* in GBM and promotes immune evasion, which reveals a mechanism underlying the inefficiency of EGFR-TKIs in *EGFR*-amplified tumors.

GBM has long been known as a "cold tumor" characterized by a lack of antitumor T cell infiltration within the TME and poor response to immunotherapies (25). The EGFR signaling pathway has been reported to play important roles in cancer immune evasion. EGFR induces PD-L1 glycosylation by up-regulating the level of B3GNT3 glycosyltransferase, which is essential for PD-L1/PD-1 interaction and T cell inactivation (20). Moreover, inhibition of EGFR induces the expression of MHC I and MHC II and promotes the pathway of antigen presentation (26). Thus, blocking EGFR improves the response to immunotherapy against PD-L1/PD-1 (27–29). Our present study identified that *SEC61G* is frequently coamplified with *EGFR* and overexpressed in GBM. While SEC61G can also up-regulate EGFR levels, we proved that the effect of SEC61G on PD-L1 expression is largely independent of the EGFR pathway. Although mouse cells with amplification of *7p11* loci are not currently available, our study revealed that depletion of SEC61G in the GL-26 mouse GBM cells induces antitumor T cell immunity and inhibits GBM tumor growth. Thus, SEC61G may act as a critical regulator for immune evasion and tumorigenesis in *EGFR*-amplified tumors.

Secreted and transmembrane proteins play key roles in immune regulation, tumor growth, and malignant transformation. The SEC61 translocon complex, composed of SEC61α/β/γ (SEC61A/B/G) heterotrimer, regulates almost all secreted and transmembrane proteins into the ER for further processing, such as glycosylation (18). As an essential component of the SEC61 translocon, SEC61G is required for the structural stability of the translocon complex and the translocation of client proteins across the ER (30–32). Studies have reported that SEC61G is up-regulated in multiple kinds of cancers (33–35), and high-level SEC61G predicts poor survival of cancer patients and resistance to chemo- and radiotherapy (36, 37). Several studies also investigated the mutual coexpression between SEC61G and EGFR in tumors and explored the intrinsic mechanisms, which include coamplification, intergenic fusion, and so on (34, 38). Targeting the SEC61 translocon has been validated to inhibit cell survival and tumor growth in preclinical studies (39, 40). A SEC61 inhibitor, KZR-261, is currently in a phase I clinical trial in patients with advanced solid tumors (NCT05047536). In addition, a most recent meeting report demonstrated that targeting SEC61 reduces PD-L1 levels in tumor cells, resulting in an increased number of $CD8^+$ T cells and improved efficiency of anti-PD-1 therapy (41). This work is consistent with our present study and strongly supports a critical role of SEC61 in tumor immune suppression, suggesting a potential for SEC61 as a target of immunotherapy.

In conclusion, our study demonstrates that *SEC61G* is coamplified with *EGFR* in GBM and promotes immune evasion by regulating the expression of ICLs. Thus, SEC61G-mediated immune evasion may act as a critical mechanism for tumorigenesis, particularly in *EGFR*-amplified tumors, and targeting SEC61G represents a potential strategy for combination therapy of *EGFR*-amplified GBMs.

Materials and Methods

Establishment of Patient-Derived GBM Cells. Fresh GBM specimens were obtained by surgical resection at the Department of Neurosurgery of Nanfang Hospital of Southern Medical University (Guangzhou, China). Tumor material was obtained with patients' informed consent as approved by the institutional review board. Tumor tissues were placed in prechilled PBS with 2% antibiotic–antimycotic (Gibco, Grand Island, NY, USA) and then repeatedly sheared with sterilized surgical scissors. The sheared tissues were transferred to a 50-mL centrifuge tube, and cell masses were separated into single cells by repeatedly blowing with a micropipette. Cell suspension was then allowed to pass through a cell filter to remove large tissues, and cells were then seeded in 25-cm^2 culture flasks and cultured in DMEM with 15% FBS. The detailed information of patients for GBM cell establishment is shown in *SI Appendix*, Table S1.

Statistical Analyses. Statistical analyses were performed with GraphPad Prism 8.0 software. Data are presented as the means ± SD or SEM. All western blot experiments were repeated at least three times unless otherwise indicated. For all representative images, results were reproduced in at least three independent experiments. For all quantitative data, the statistical test used is indicated in the figure legends. We assessed differences in the human GBM data using the Pearson correlation test, the in vitro data between two groups (=2 groups) using the two-tailed Student's *t* test, the in vitro data among multiple groups (>2 groups), and the in vivo data using two-way ANOVA. We considered $P < 0.05$ to be significant.

Study Approval. All animal experiments were approved by the Institutional Animal Care and Use Committee of Southern Medical University. The detailed

methods for antibodies and reagents, cell culture, transfection and treatment, plasmid construction, siRNA, qPCR, immunofluorescence and immunohistochemical analysis, T cell–mediated tumor cell killing assays, cellular ubiquitination assays, and animal experiments are described in *SI Appendix*.

Ethics Approval and Consent to Participate. All aspects of this study were approved by the Institutional Research Ethics Committee of Southern Medical University.

Data, Materials, and Software Availability. All study data are included in the article and/or *SI Appendix*.

ACKNOWLEDGMENTS. This work was supported by the Natural Science Foundation of Guangdong Province (2023A1515010419, 2021A1515011067), National Natural Science Foundation of China (Grants 31871406), and Guangdong Provincial High-Level University Construction Funds.

Author affiliations: [a]Department of Cell Biology, School of Basic Medical Science, Southern Medical University, Guangzhou 510515, China; [b]Department of Radiation Oncology, Zhujiang Hospital, Southern Medical University, Guangzhou 510285, China; [c]Guangdong Province Key Laboratory of Molecular Tumor Pathology, School of Basic Medical Science, Southern Medical University, Guangzhou 510515, China; and [d]Department of Neurosurgery, Nanfang Hospital, Southern Medical University, Guangzhou 510515, China

1. O. Rominiyi *et al.*, Tumour treating fields therapy for glioblastoma: Current advances and future directions. *Br. J. Cancer* **124**, 697–709 (2021).
2. L. L. Li *et al.*, Critical role of lncEPAT in coupling dysregulated EGFR pathway and histone H2A deubiquitination during glioblastoma tumorigenesis. *Sci. Adv.* **8**, eabn2571 (2022).
3. P. C. Pan, R. S. Magge, Mechanisms of EGFR Resistance in Glioblastoma. *Int. J. Mol. Sci.* **21**, 8471 (2020).
4. Y. A. Yabo, S. P. Niclou, A. Golebiewska, Cancer cell heterogeneity and plasticity: A paradigm shift in glioblastoma. *Neuro Oncol.* **24**, 669–682 (2022).
5. Z. An, O. Aksoy, T. Zheng, Q. W. Fan, W. A. Weiss, Epidermal growth factor receptor and EGFRvIII in glioblastoma: Signaling pathways and targeted therapies. *Oncogene* **37**, 1561–1575 (2018).
6. G. Guo *et al.*, A TNF-JNK-Axl-ERK signaling axis mediates primary resistance to EGFR inhibition in glioblastoma. *Nat. Neurosci.* **20**, 1074–1084 (2017).
7. C. M. Jackson, J. Choi, M. Lim, Mechanisms of immunotherapy resistance: Lessons from glioblastoma. *Nat. Immunol.* **20**, 1100–1109 (2019).
8. A. R. Pombo Antunes *et al.*, Understanding the glioblastoma immune microenvironment as basis for the development of new immunotherapeutic strategies. *Elife* **9**, e52176 (2020).
9. M. Zhan *et al.*, CD155 in tumor progression and targeted therapy. *Cancer Lett.* **545**, 215830 (2022).
10. C. W. Li *et al.*, Glycosylation and stabilization of programmed death ligand-1 suppresses T-cell activity. *Nat. Commun.* **7**, 12632 (2016).
11. P. Zhang *et al.*, Crystal structure of CD155 and electron microscopic studies of its complexes with polioviruses. *Proc. Natl. Acad. Sci. U.S.A.* **105**, 18284–18289 (2008).
12. Y. Xu *et al.*, PD-L2 glycosylation promotes immune evasion and predicts anti-EGFR efficacy. *J. Immunother. Cancer* **9**, e002699 (2021).
13. Y. Liu *et al.*, Deletions linked to TP53 loss drive cancer through p53-independent mechanisms. *Nature* **531**, 471–475 (2016).
14. Y. H. Liu *et al.*, Targeting 17q23 amplicon to overcome the resistance to anti-HER2 therapy in HER2+breast cancer. *Nat. Commun.* **9**, 4718 (2018).
15. M. Chen *et al.*, An epigenetic mechanism underlying chromosome 17p deletion-driven tumorigenesis. *Cancer Discov.* **11**, 194–207 (2021).
16. M. Linxweiler, B. Schick, R. Zimmermann, Let's talk about Secs: Sec61, Sec62 and Sec63 in signal transduction, oncology and personalized medicine. *Signal Transduct. Target. Ther.* **2**, 17002 (2017).
17. H. A. Yang *et al.*, EGFR amplification is a putative resistance mechanism for NSCLC-LM patients with TKI therapy and is associated with poor outcome. *Front. Oncol.* **12**, 902664 (2022).
18. C. Xu, D. T. Ng, Glycosylation-directed quality control of protein folding. *Nat. Rev. Mol. Cell Biol.* **16**, 742–752 (2015).
19. S. Q. Xu *et al.*, Sec61 gamma is a vital protein in the endoplasmic reticulum membrane promoting tumor metastasis and invasion in lung adenocarcinoma. *Br. J. Cancer* **128**, 1478–1490 (2023).
20. C. W. Li *et al.*, Eradication of triple-negative breast cancer cells by targeting glycosylated PD-L1. *Cancer Cell* **33**, 187–201.e10 (2018).
21. B. C. Cross *et al.*, Eeyarestatin I inhibits Sec61-mediated protein translocation at the endoplasmic reticulum. *J. Cell Sci.* **122**, 4393–4400 (2009).
22. R. Bagheri-Yarmand *et al.*, Combinations of tyrosine kinase inhibitor and ERAD inhibitor promote oxidative stress-induced apoptosis through ATF4 and KLF9 in medullary thyroid cancer. *Mol. Cancer Res.* **17**, 751–760 (2019).
23. Q. Wang *et al.*, ERAD inhibitors integrate ER stress with an epigenetic mechanism to activate BH3-only protein NOXA in cancer cells. *Proc. Natl. Acad. Sci. U.S.A.* **106**, 2200–2205 (2009).
24. N. Singh, R. Joshi, K. Komurov, HER2-mTOR signaling-driven breast cancer cells require ER-associated degradation to survive. *Sci. Signal.* **8**, ra52 (2015).
25. S. C. Frederico *et al.*, Making a cold tumor hot: The role of vaccines in the treatment of glioblastoma. *Front. Oncol.* **11**, 672508 (2021).
26. B. P. Pollack, B. Sapkota, T. V. Cartee, Epidermal growth factor receptor inhibition augments the expression of MHC class I and II genes. *Clin. Cancer Res.* **17**, 4400–4413 (2011).
27. E. Sugiyama *et al.*, Blockade of EGFR improves responsiveness to PD-1 blockade in EGFR-mutated non-small cell lung cancer. *Sci Immunol.* **5**, eaav3937 (2020).
28. E. A. Akbay *et al.*, Activation of the PD-1 pathway contributes to immune escape in EGFR-driven lung tumors. *Cancer Discov.* **3**, 1355–1363 (2013).
29. C. Dominguez, K. Y. Tsang, C. Palena, Short-term EGFR blockade enhances immune-mediated cytotoxicity of EGFR mutant lung cancer cells: Rationale for combination therapies. *Cell Death Dis.* **7**, e2380 (2016).
30. D. Falcone *et al.*, Stability and function of the Sec61 translocation complex depends on the Sss1p tail-anchor sequence. *Biochem. J.* **436**, 291–303 (2011).
31. J. A. Lycklama a Nijeholt, J. de Keyzer, I. Prabudiansyah, A. J. M. Driessen, Characterization of the supporting role of SecE in protein translocation. *FEBS Lett.* **587**, 3083–3088 (2013).
32. Y. Esnault, D. Feldheim, M. O. Blondel, R. Schekman, F. Kepes, SSS1 encodes a stabilizing component of the Sec61 subcomplex of the yeast protein translocation apparatus. *J. Biol. Chem.* **269**, 27478–27485 (1994).
33. J. Ma *et al.*, SEC61G promotes breast cancer development and metastasis via modulating glycolysis and is transcriptionally regulated by E2F1. *Cell Death Dis.* **12**, 550 (2021).
34. Z. Lu *et al.*, Glioblastoma proto-oncogene SEC61gamma is required for tumor cell survival and response to endoplasmic reticulum stress. *Cancer Res.* **69**, 9105–9111 (2009).
35. H. Gao *et al.*, SEC61G plays an oncogenic role in hepatocellular carcinoma cells. *Cell Cycle* **19**, 3348–3361 (2020).
36. T. Lu *et al.*, SEC61G overexpression and DNA amplification correlates with prognosis and immune cell infiltration in head and neck squamous cell carcinoma. *Cancer Med.* **10**, 7847–7862 (2021).
37. B. Liu *et al.*, Identification of SEC61G as a novel prognostic marker for predicting survival and response to therapies in patients with glioblastoma. *Med. Sci. Monitor.* **25**, 3624–3635 (2019).
38. T. Servidei *et al.*, Novel SEC61G-EGFR fusion gene in pediatric ependymomas discovered by clonal expansion of stem cells in absence of exogenous mitogens. *Cancer Res.* **77**, 5860–5872 (2017).
39. A. Domenger *et al.*, The Sec61 translocon is a therapeutic vulnerability in multiple myeloma. *EMBO Mol. Med.* **14**, e14740 (2022).
40. A. O. Paatero *et al.*, Apratoxin kills cells by direct blockade of the Sec61 protein translocation channel. *Cell Chem. Biol.* **23**, 561–566 (2016).
41. J. A. Whang, A. Fan, J. Jiang, C. J. Kirk, T. Muchamuel, Sec61 inhibitor KZR-834, an anti-cancer agent, exhibits immunomodulatory activity and combines with PD-1 blockade to further enhance immune responses. *Cancer Res.* **82**, 5592 (2022).